

Magnetic and structural behaviour of $\text{Nd}_2\text{Fe}_{14}\text{B}/\alpha\text{-Fe}$ and $(\text{NdDy})_2\text{Fe}_{14}\text{B}/\alpha\text{-Fe}$ obtained by mechanical milling and annealing

S. GUTOIU, E. DOROLTI, O. ISNARD^a, I. CHICINAȘ^b, V. POP^{*}

Faculty of Physics, Babes-Bolyai University, 400084 Cluj-Napoca, Romania

^aInstitut Néel, CNRS, University Joseph Fourier de Grenoble, BP 166X, 38042 Grenoble, Cédex 9, France

^bMaterials Sciences and Technology Dept., Technical University of Cluj-Napoca, 103-105 Muncii ave., 400641 Cluj-Napoca, Romania

Two type of nanocomposite $\text{Nd}_2\text{Fe}_{14}\text{B}+10$ wt % $\alpha\text{-Fe}$ and $(\text{Nd}_{0.92}\text{Dy}_{0.08})_2\text{Fe}_{14}\text{B}+22$ wt % $\alpha\text{-Fe}$ were prepared by high energy ball milling and subsequent annealing under high vacuum at different temperatures and annealing times. X-ray diffraction followed by electron microscopy were used to evidenced the evolution of the structure and microstructure of the samples. The width of the diffraction peaks of the hard magnetic phase increases with milling times and disappears after 12 h of milling. The remanent magnetisation, the coercive field and the exchange coupling between the hard and the soft magnetic phases were deduced from room temperature magnetic hysteresis loops, performed in magnetic fields up to 10 T.

(Received September 4, 2010; accepted October 14, 2010)

Keywords: Soft/hard nanocomposite, Mechanical milling, Exchange-coupling, Coercivity

1. Introduction

At the beginning of 1991, Kneller et al. [1] showed that a mixture of hard ($\text{Nd}_2\text{Fe}_{14}\text{B}$) and soft (Fe_3B or αFe) nanograins phases could lead to exchange coupled nanocomposites. The maximum energy product obtained experimentally for this type of nanocomposites was 200 kJ/m^3 [2]. Therefore, a discrepancy between the experimental value of this maximum energy product and the theoretic value of 300 kJ/m^3 was observed [3]. This difference was explained by the weakness of the exchange interactions between nanograins [4, 5]. The exchange coupling is strongly influenced by structure and microstructure [1]. The ratio between the hard and soft magnetic phases as well as the substitution by different elements plays an important role in interphase exchange coupling [6, 7]. Theoretical studies [1, 8] show that the microstructure of the sample, especially the crystallite size of the soft phase, plays an essential role in magnetic properties of the materials. For a successful coupling between the soft phase and hard magnetic phase, the crystallite size of the soft phase should be smaller than the double of the domain wall width of the hard phase. The experimental criteria for the presence of exchange mechanism are given by the high reversibility of the demagnetization curve and by the enhanced remanence ($M_r/M_s > 0.5$).

Until now, mainly two types of $\text{Nd}_2\text{Fe}_{14}\text{B}$ -based nanocomposite magnets, obtained by different techniques, have been widely studied: $\alpha\text{-Fe}/\text{Nd}_2\text{Fe}_{14}\text{B}$ [7, 9, 10] and $\text{Fe}_3\text{B}/\text{Nd}_2\text{Fe}_{14}\text{B}$ [11, 12]. For $\alpha\text{-Fe}/\text{Nd}_2\text{Fe}_{14}\text{B}$, remanence enhancement was observed by Coehoorn [13] in rapidly quenched Nd-Fe-B ribbons. Using the same technique Hirose et al. [11] succeeds to obtain $\text{Fe}_3\text{B}/\text{Nd}_2\text{Fe}_{14}\text{B}$

phase nanocomposites. Dy substitution for Nd has been successfully used to enhance the coercivity in sintered $(\text{Nd}_{0.5}\text{Dy}_{0.5})_{15}\text{Fe}_{77}\text{B}_8$ magnet [14]. However, for mechanically milled nanocomposites, the substitution of a small amount of Nd by Dy does not affect the magnetic properties of the nanocomposite [10]. The main reason is that Dy substitution results in an increase of the crystallization temperature, which in turn requires a higher annealing temperature, and thus promotes excessive grain growth for the soft phases and leads to an undesirable coarse microstructure [15]. The refinement of the microstructure becomes the key factor for the enhancement of the magnetic properties in soft/hard coupled nanocomposite magnets. Miao et al. [6] shows that an improvement of the enhanced remanence from 0.56 to 0.64 is realized by increasing the fraction of $\alpha\text{-Fe}$ from 14% to 73% in the nanocomposite of $\text{Nd}_{2x}\text{Fe}_{100-3x}\text{B}_x$. Another important parameter for a magnetic material is the Curie temperature. Lewis et al. [16] investigated the dependence of Curie temperatures on the percentage of Fe from melt-spun nanocomposite of $\text{Nd}_2\text{Fe}_{14}\text{B} + x$ wt% Fe ($x = 1, 14, 18$ and 27 wt %). Thus magnetic measurements highlighted an increasing Curie temperature with 18 degree for $\text{Nd}_2\text{Fe}_{14}\text{B} + 27$ wt % Fe nanocomposite compared to hard magnetic phase $\text{Nd}_2\text{Fe}_{14}\text{B}$. Rada et al. [7] shows that the increase of the soft magnetic phase percentage, in mechanically milled $\text{Nd}_2\text{Fe}_{14}\text{B}+x\%$ Fe ($x = 10, 25, 35$ wt %) nanocomposite, improves the corrosion resistance in slightly acidic environment.

One way to improve magnetic properties and exchange coupling between the hard and soft magnetic phases is the optimization of annealing conditions. In mechanically milled samples, a lot of defects and internal stresses could be removed by annealing. The restoration of

the crystalline structure of the hard phase by annealing is an important factor in increasing of the coercivity. For this type of composites, the recrystallization temperature of soft magnetic phase is smaller than the recrystallization temperature of hard magnetic phases. Consequently the refinement of the hard phase structure by annealing will come along with an undesirable increase of soft crystallite dimension. In rapidly quenched alloys, Bernardi et al. [12] states that in order to suppress the formation of soft phases, the samples must be annealed at a heating rate of 15–25°/s. A high heating rate of about 50°/s or more usually led to the formation of large α Fe grains. The mechanism responsible for the favoured growth of α Fe is not explained. One of the solutions could be a flash annealing for a time of 1 to 120 seconds [12].

Recently, by mechanical milling and annealing, we have successfully obtained hard/soft type magnetic nanocomposite with coercivity in a range of 3.7 – 8.2 kOe [10, 17, 18]. A few percent of Dy, substituted for Nd in the Nd-Fe-B hard magnetic phase proved to refine the microstructure and enhance the anisotropy field [14, 19, 20]. This increase of magnetic anisotropy favours an improvement of the coercivity. However, the presence of Dy decreases the saturation magnetization substantially as a consequence of the antiparallel coupling between Fe and Dy moments. Having in mind these two complementary influences (coercive and remanence) of the substitution of Nd by Dy, we propose a comparative study concerning the effect of the amount of the soft magnetic phases on the exchange coupling.

2. Experimental

The mixture of 78wt% $(\text{Nd}_{0.92}\text{Dy}_{0.08})_2\text{Fe}_{14}\text{B}/22\text{wt}\% \alpha\text{-Fe}$ and 90% $\text{Nd}_2\text{Fe}_{14}\text{B}/10\text{wt}\% \alpha\text{-Fe}$ was mechanically milled under argon atmosphere in a high-energy planetary mill. Several milling times were used ranging from 4 to 12 hours. The microstructure was tailored by appropriate heat treatments under vacuum between 450 and 800 °C from 5 min to 14 hours. More experimental details concerning the sample preparation are given elsewhere [10]. X-ray diffraction (XRD) was carried out on a Bruker D8 Advance diffractometer with $\text{Cu K}\alpha$ radiation and a Siemens D500 powder diffractometer using the $K_{\alpha 1}$ radiation of copper ($\lambda = 0.15406$ nm) in the angular interval $2\theta = 20$ to 90° . The microstructures of the samples were investigated using XRD and scanning electron microscopy (SEM). The hysteresis curves were recorded at room temperature by the extraction method in a continuous magnetic field of up to 10 T and by a vibrating sample magnetometer using the same maximum applied field.

3. Results and discussion

The diffraction patterns obtained for 90 wt % $\text{Nd}_2\text{Fe}_{14}\text{B}/10$ wt % $\alpha\text{-Fe}$ nanocomposites are plotted in fig. 1. The X-ray diffraction pattern of hard magnetic phase milled for 2 hours is also shown for comparison. From figure 1a, which presenting diffraction patterns of the as-milled sample, we can see that for long milling times the

diffraction peaks corresponding to the hard magnetic phases (see the correspondent 2:14:1 bars phases on figure 1a) become undetectable. This disappearance of the diffraction peaks can be explained by several effects: the amorphisation of the hard phase structure by milling, a decrease of the crystallites sizes and the occurrence of induced internal stresses. The alpha iron structure is less sensitive to the above factors, consequently the $\alpha\text{-Fe}$ diffraction peak remains detectable during the milling processes. The characteristic diffraction peaks of hard magnetic phase are restored by a heat treatment (figure 1b). After annealing at 550 °C for 1.5 hours, the width of the diffraction peaks decreases in comparison to the corresponding milled samples. This behaviour could be given by diminish of the second-order internal stresses and of the defects density. For long milling times, the heat treatment at 550 °C does not succeed to remove all defects and stresses induced by milling and consequently do not lead to the appearance of the $\text{Nd}_2\text{Fe}_{14}\text{B}$ characteristic diffraction peaks. This behaviour can be a drawback for the hard/soft magnetic exchange coupling process.

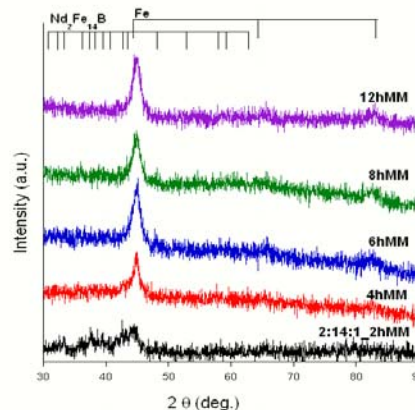


Fig. 1a. X-ray diffraction patterns of the $\text{Nd}_2\text{Fe}_{14}\text{B}+10$ wt% $\alpha\text{-Fe}$ composites milled from 4 to 12 h in comparison to that of $\text{Nd}_2\text{Fe}_{14}\text{B}$ hard phase milled for 2 h.

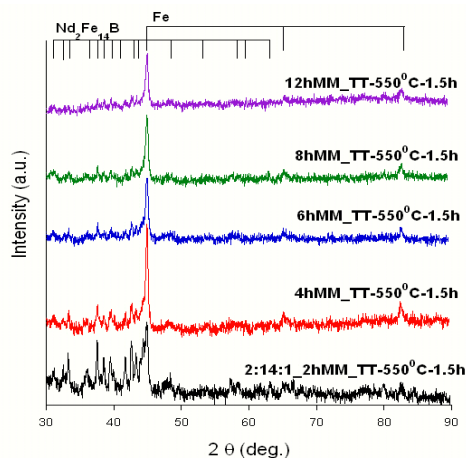


Fig. 1b. X-ray diffraction patterns of the $\text{Nd}_2\text{Fe}_{14}\text{B}+10$ wt% $\alpha\text{-Fe}$ composites milled from 4 to 12 h and annealed at 550°C for 1.5 h, in comparison to that of $\text{Nd}_2\text{Fe}_{14}\text{B}$ hard phase milled for 2 h annealed in the same conditions.

Chemical and microstructure characterization images obtained by SEM+EDX for $\text{Nd}_2\text{Fe}_{14}\text{B}+10\text{wt}\%$ $\alpha\text{-Fe}$ nanocomposite, mechanically milled for 4 and annealed at 550°C for 1.5 hours are presented in fig. 2. The particles distribution is rather large. Each particle is formed by clusters of the different crystallites. The maps of elements distribution, obtained by EDX, show a homogenous distribution of the elements in the powder. These results prove that after 4 hours of milling, followed by an annealing at 550°C for 1.5 hours, the hard and soft phases are well mixed.

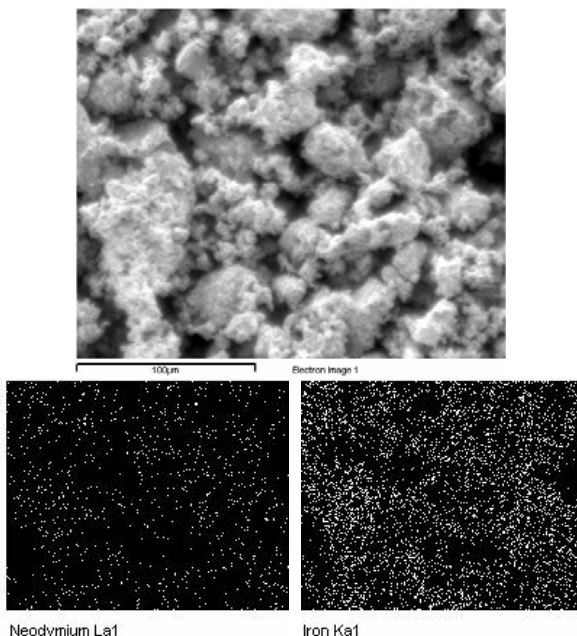


Fig. 2. SEM picture (a) and elements distribution maps (EDX) results (b) of $\text{Nd}_2\text{Fe}_{14}\text{B}+10\text{ wt}\%$ Fe milled for 4 h and annealed at 550°C for 1.5 h.

X-ray diffraction pattern of $(\text{Nd}_{0.92}\text{Dy}_{0.08})_2\text{Fe}_{14}\text{B}/\alpha\text{-Fe}$ samples milled for 4, 6, 8 and 12 hours are presented in figure 3a. The width of the diffraction peaks increases by increasing milling time and almost disappear for long milling times, following a similar behaviour with $\text{Nd}_2\text{Fe}_{14}\text{B}/\alpha\text{-Fe}$ samples. An annealing at 550°C for 1.5 hours diminishes the number of defects and the internal stresses by local diffusion (annealing temperature is lower than recrystallization temperature). As consequently, the characteristic diffraction peaks for the two phases are well evidenced in annealed samples, figure 3b. The XRD patterns show also that no oxides were occurred during the milling or annealing. The nanocrystallites mean sizes of $\alpha\text{-Fe}$, calculated from Full-Width-at-Half-Maximum, FWHM, of the diffraction peak $2\theta\approx 82.5^\circ$, according to Scherrer's formula [21], for $(\text{Nd}_{0.92}\text{Dy}_{0.08})_2\text{Fe}_{14}\text{B}/\alpha\text{-Fe}$ samples milled for 6 h and annealed at different temperatures, are given in table 1. For annealing temperatures higher than 450°C , the second-order internal stresses were removed; consequently, their contribution to the FWHM was neglected. By increasing the annealing time, the crystallite sizes increase. The big crystallites obtained after annealing at 650 and 800°C result from the

recrystallization process which take place for this annealing temperatures. The smaller crystallite sizes obtained for sample annealed at 450°C can result from the fact that for these annealing conditions the recrystallization process has not yet begun.

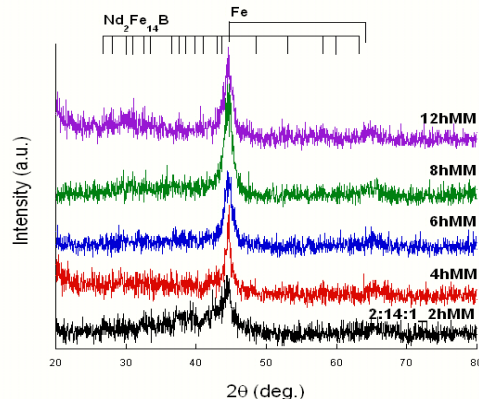


Fig. 3a. X-ray diffraction patterns of the $(\text{Nd}_{0.92}\text{Dy}_{0.08})_2\text{Fe}_{14}\text{B} + 22\text{wt}\%$ $\alpha\text{-Fe}$ composite samples milled from 4 to 12 h in comparison to that of $(\text{Nd}_{0.92}\text{Dy}_{0.08})_2\text{Fe}_{14}\text{B}$ milled for 2 h.

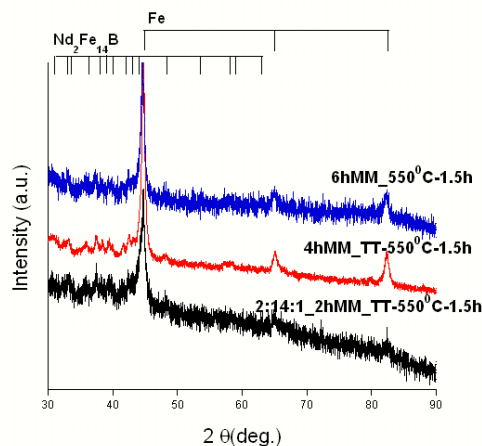


Fig. 3b. X-ray diffraction patterns of the $(\text{Nd}_{0.92}\text{Dy}_{0.08})_2\text{Fe}_{14}\text{B} + 22\text{wt}\%$ $\alpha\text{-Fe}$ composite samples milled from 6 and 8 h and annealed for time and temperature indicated in comparison to that of pure $(\text{Nd}_{0.92}\text{Dy}_{0.08})_2\text{Fe}_{14}\text{B}$ milled for 2 h and annealed in the same conditions.

Table 1. The nanocrystallites mean sizes, D , of $\alpha\text{-Fe}$, for $(\text{Nd}_{0.92}\text{Dy}_{0.08})_2\text{Fe}_{14}\text{B}/\alpha\text{-Fe}$ samples milled for 6 h and annealed at different temperature for 1.5h.

Annealing temperature ($^\circ\text{C}$)	FWHM (rad)	D (nm)
450.00	0.0135	13.600
550.00	0.0102	18.000
650.00	0.0048	38.300
800.00*	0.0035	52.100

* annealed for 5 minutes

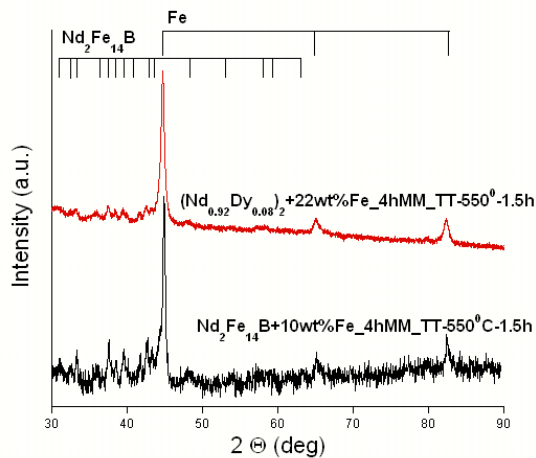


Fig. 4. X-ray diffraction patterns of $\text{Nd}_2\text{Fe}_{14}\text{B} + 10 \text{ wt}\%$ Fe and of $(\text{Nd}_{0.92}\text{Dy}_{0.08})_2\text{Fe}_{14}\text{B} + 22 \text{ wt}\%$ Fe mechanically milled for 4 h and annealed at 550°C for 1.5 h.

XRD patterns for composites with 10 and 22 wt% Fe milled 4 hours and annealed at 550°C for 1.5 hours are given in figure 4. The annealing induced improvement of crystallinity of the hard magnetic phase is better realised in samples with less $\alpha\text{-Fe}$ content. This behaviour can explain the magnetic evolution of our composite for the higher amount of iron.

The magnetic hysteresis loops for as milled $\text{Nd}_2\text{Fe}_{14}\text{B} + 10 \text{ wt}\%$ $\alpha\text{-Fe}$ nanocomposite (Figure 5a) show a nanocomposite powder with very low coercivity. A heat treatment at 550°C for 1.5 hours increases the magnetic hardening of the composite and coercivity reach the highest value of 0.58 T for 4 hours of milling. In the same time the demagnetisation curve for this sample present a shoulder, which results in weakness of the remanence, proving a poor exchange coupling between hard and soft magnetic phases. The effect of annealing is more obvious for the longer milling times, where the hard and soft magnetic phases are intimately mixed and the crystallite sizes are in nanometre region. The best exchange coupling, for the above annealed nanocomposites is observed for the sample mechanically milled for 6 hours (fig. 5b).

The influence of the annealing on the coercivity and remanence of 22 wt% of iron samples $(\text{Nd}_{0.92}\text{Dy}_{0.08})_2\text{Fe}_{14}\text{B}/\alpha\text{-Fe}$, is similar to that evidenced in Fig. 5 for $\text{Nd}_2\text{Fe}_{14}\text{B} + 10 \text{ wt}\%$ $\alpha\text{-Fe}$ nanocomposite [10]. An appropriate annealing temperature will increase the coercivity respectively the exchange coupling between the hard and soft magnetic phases.

To compare the effect of the iron amount on the hardness of the coupling between the two phases, the hysteresis loops of $(\text{Nd}_{0.92}\text{Dy}_{0.08})_2\text{Fe}_{14}\text{B} + 22 \text{ wt}\%$ $\alpha\text{-Fe}$ and $\text{Nd}_2\text{Fe}_{14}\text{B} + 10 \text{ wt}\%$ $\alpha\text{-Fe}$ nanocomposites are given for comparison, figure 6. The hysteresis cycles for the sample with 10 wt% Fe presented a shoulder which may indicate a partial uncoupling between the hard and soft phases. The

M_r/M_s values show a poor magnetic hardness of Fe by the hard phase.

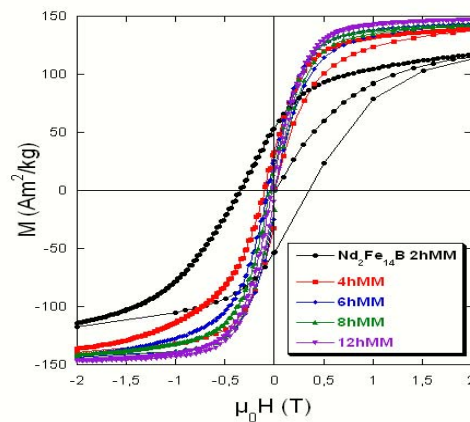


Fig. 5a Room temperature hysteresis loops recorded for $\text{Nd}_2\text{Fe}_{14}\text{B} + 10 \text{ wt}\%$ $\alpha\text{-Fe}$ nanocomposite milled between 4 and 12 h compared to $\text{Nd}_2\text{Fe}_{14}\text{B}$ hard phase milled for 2 h

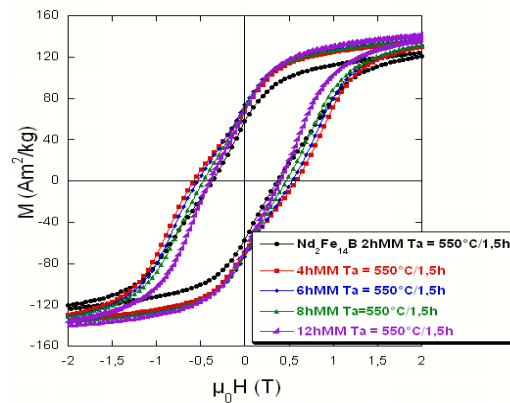


Fig. 5b Room temperature hysteresis loops recorded for $\text{Nd}_2\text{Fe}_{14}\text{B} + 10 \text{ wt}\%$ $\alpha\text{-Fe}$ nanocomposite milled between 4 and 12 hours and annealed for the indicated time and temperature compared to that of $\text{Nd}_2\text{Fe}_{14}\text{B}$ milled for 2 h annealed in the same conditions.

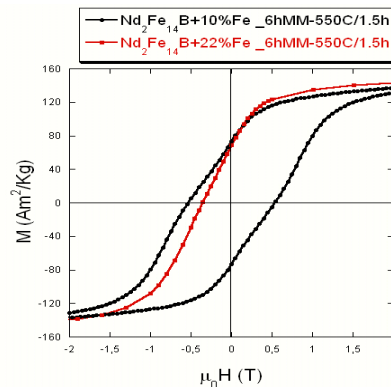


Fig. 6. Room temperature hysteresis cycles recorded for $(\text{Nd}_{0.92}\text{Dy}_{0.08})_2\text{Fe}_{14}\text{B} + 22 \text{ wt}\%$ $\alpha\text{-Fe}$ and $\text{Nd}_2\text{Fe}_{14}\text{B} + 10 \text{ wt}\%$ $\alpha\text{-Fe}$ nanocomposites milled for 6 h annealed at 550°C for 1.5 h.

The evolution of the exchange coupling and of the coercivity is well given by the derivative dM/dH vs. magnetic field (figure 7). It is obvious that, for the above preparation conditions, even the inter-phases exchange coupling is not entirely fulfilled, 10% of iron is more appropriate to obtain better coercivity and remanence. This effect may be due to the milling and annealing (mainly annealing) conditions. For the nanocomposite with 22 wt% of iron the corresponding peak dM/dH is broad. This behaviour can be understood by a large distribution of α -Fe size grains, which will result in a large distribution of coercive hardness of the soft/hard composite. In comparison, the figure corresponding to 10 wt% of iron shows two narrower peaks. The first one, at low field, correspond to the non coupled α -Fe crystallites and the second one, at about 0.8 T correspond to the exchange coupled soft/hard composite. This behaviour proves better magnetic properties for lower Fe contents, but also a weakness in the preparation of this composite which results in a non negligible quantity of iron uncoupled to the hard phase.

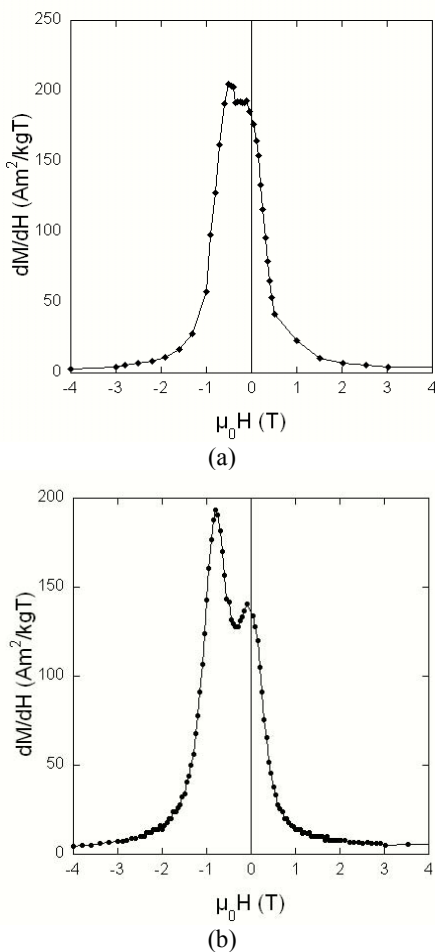


Fig. 7. dM/dH vs. H curves of $(Nd_{0.92}Dy_{0.08})_2Fe_{14}B + 22$ wt% Fe (a) and $Nd_2Fe_{14}B + 10$ wt% Fe (b) mechanically milled for 6 hours and annealed at $550^\circ C$ for 1.5 h.

4. Conclusions

Mechanical milling has been applied in order to obtain $Nd_2Fe_{14}B/\alpha Fe$ and $(Nd_{0.92}Dy_{0.08})_2Fe_{14}B/\alpha Fe$ magnetic nanocomposites. The influence of the milling and annealing conditions on the microstructure and magnetic behaviours of the milled powder have been studied. Long milling times induce defects, decrease the crystallites size and induce large microstrains. By increasing the milling time we decrease the coercivity by destroying the crystallinity of hard phase. Annealing at appropriate temperatures, lower than the recrystallization temperature, diminishes the defects and reduce the internal stresses, consequently the coercivity and the remanence of the soft/hard magnetic nanocomposite are considerably improved. The strength of the exchange coupling between the hard and the soft magnetic nanocrystallites can be improved by adjusting the amount of the soft magnetic phase and for a given iron content by changing the milling and/or annealing conditions. Higher amounts of iron will disfavour the recovery, by annealing, of the optimum microstructure of hard magnetic phase damaged by milling. In the same time a higher annealing temperature will increase the size of the soft magnetic crystallites. This increase will decrease the exchange coupling between the two phases. For 10% of iron we succeed to have better magnetic properties, but we still have an important amount of soft magnetic phase remains uncoupled to the hard phase. Further investigations on the milling and annealing conditions are envisaged in order to maximise the efficiency of soft/hard interphase exchange coupling. More deep studies are scheduled for a better determination of the stress and defect density.

Acknowledgements

This work has been partly supported by Romanian Ministry of Education, grant PNCD II 72-186/2008

References

- [1] E.F. Kneller, R. Hawig, IEEE Trans. Magn. **27**, 3588 (1991).
- [2] J. Bauer, M. Seeger, A. Zern, H. Kronmüller, J. Appl. Phys. **80**, 1667 (1996)
- [3] H. Fukunaga, J. Kuma, Y. Kanai, IEEE Trans. Magn. **35**, 3235 (1999)
- [4] H. Fukunaga, N. Kitajima, Y. Kanai, Mater. Trans., Jpn. Trans. Metals **37**, 864 (1996)
- [5] H. Fukunaga, Y. Kanai, in Proc. 10th Intern. Symposium on Magnetic Anisotropy and Coercivity in Rare-Earth Transition Metal Alloys, Werkstoff-Informationsgesellschaft, Dresden, Germany 1998, p. 237,
- [6] W.F. Miao, J. Ding, P.G. McCormick, R. Street, J. Alloys Compounds **240**, 200 (1996)
- [7] M. Rada, J. Lyubina, A. Gebert, O. Gutfleisch, L. Schultz, J. Mag. Mat., **290-291**, 1251 (2005)
- [8] R. Skomski, J. Appl. Phys. **76**, 7059 (1994).

- [9] A. Manat, R.A. Buckley, H.A. Davis, *J. Mag. Mag. Mat.* **128**, 302 (1993).
- [10] E. Dorolti, V. Pop, O. Isnard, D. Givord, I. Chicinas, *J. Optoelectron. Adv. Mater.* **9**, 1474 (2007).
- [11] S. Hirosawa, Y. Shigemoto, T. Miyoshi, H. Kanekiyo, *Scripta Materialia* **48**, 839 (2003).
- [12] J. Bernardi, T. Schrefl, J. Fidler, Th. Rijks, K. de Kort, V. Archambault, D. Pere, S. David, D. Givord, J. F. O'Sullivan, P. A. I. Smith, J. M. D. Coey, U. Czernik, M. Gronefeld, *J. Mag. Mag. Mat.* **219**, 186 (2000).
- [13] R. Coehoorn, D. B. Mooij, J. P. W. B. Duchateau, K. H. J. Buschow, *J. Phys. C* **49**, 669 (1998).
- [14] M. Sagawa, S. Hirosawa, K. Tokuhara, *J. Appl. Phys.* **61**, 3559 (1987).
- [15] G. C. Hadjipanayis, L. Withanawasam, R. F. Krause, *IEEE Trans. Magn.* **31**, 3596 (1995).
- [16] L. H. Lewis, D. O. Welch, V. Panchanathan, *J. Mag. Mag. Mat.*, **175**, 275-278 (1997)
- [17] V. Pop, O. Isnard, I. Chicinas, D. Givord, J. M. Le Breton, *J. Optoelectron Adv Mater* **8**, 494 (2006)
- [18] V. Pop, O. Isnard, I. Chicinas, D. Givord, *J. Mag. Mag. Mat.* **310**, 2489 (2007)
- [19] Z. Liu, H. A. Davies, *J. Mag. Mag. Mater*, **290-291**, 1230 (2005)
- [20] B. E. Meacham, D. J. Branagan, J. E. Shield, *J. Magn. Mater.*, **277**, 123-129 (2004)
- [21] P. Scherrer, *Göt. Nachr.* **2**, 98 (1918)

*Corresponding author: viorel.pop@phys.ubbcluj.ro